Journal of Catalysis **202,** 78–88 (2001)
doi:10.1006/jcat.2001.3271, available online at http://www.idealibrary.com on IDEAL®

Direct Aromatic C–N Bond Cleavage Evidenced in the Hydrodenitrogenation of 2,6-Dimethylaniline over Cobalt-Promoted Mo/Al_2O_3 Sulfide Catalysts: A Reactivity and FT-IR Study

J. van Gestel,[1] C. Dujardin, F. Maugé, and J. C. Duchet

Laboratoire Catalyse et Spectrochimie, UMR CNRS 6506, ISMRA-Université, 6, Boulevard Maréchal Juin, 14050 Caen, France

Received December 12, 2000; revised March 23, 2001; accepted May 7, 2001

The hydrodenitrogenation of 2,6-dimethylaniline (DMA) was studied over a series of sulfided Co(0–4.7%)–Mo(8.7%)/Al_2O_3 catalysts at 573 K under 4 MPa total pressure and 0–56 kPa H_2S partial pressure. Two NiMo samples were tested for comparison. The reaction network presents three parallel routes: dearomatization of DMA followed by either hydrogenation–elimination to dimethylcyclohexenes and dimethylcyclohexanes, or NH_3 elimination to *m*-xylene, and disproportionation of DMA to 2-methylaniline and 2,4,6-trimethylaniline. We demonstrate that part of the xylene is formed by direct aromatic carbon–nitrogen bond cleavage through a nucleophilic substitution involving hydride species. On CoMo catalysts, in the presence of H_2S, the amount of extra xylene is independent of Co content, while the dearomatization is promoted. Without H_2S, this special substitution reaction is most important on the Mo catalyst, and strikingly Co acts as a poison. FT-IR spectroscopy of adsorbed carbon monoxide evidences a new type of sites on the sulfided catalysts after a mild hydrogen treatment. We propose that a site configuration located exclusively on unpromoted Mo atoms highly depleted in sulfur is responsible for the direct denitrogenation route. The NiMo couple behaves differently: xylene formation is independent of Ni content, which means that the specific Mo sites for direct C–N bond rupture are poisoned by nickel, even in the presence of H_2S. The location of Co and Ni on the MoS_2 slabs then appears different. © 2001 Academic Press

Key Words: **hydrodenitrogenation; sulfide catalysts; dimethylaniline; mechanism; active sites; CO; IR spectroscopy.**

INTRODUCTION

Hydrotreating on sulfide catalysts is studied mostly in the presence of H_2S in order to simulate industrial HDS conditions. The catalysts are then evaluated on the basis of the reactivity of sulfur model molecules, classically thiophene and dibenzothiophene (1, 2). However, the full potential of the bare surface of the catalyst cannot be explored in this way since conversion of the model molecule produces H_2S, which readily saturates the coordinatively unsaturated sites (CUS) exposed on the surface. In this respect, a nitrogen-containing model molecule is more appropriate to assess the ultimate potential of the catalyst because the released ammonia is believed to leave unchanged the surface of the sulfide catalyst. Quinoline is the typical nitrogen model compound but, due to the complexity of the reaction scheme, the reactivity for the individual reaction steps is difficult to assess (3, 4). Therefore, we have chosen an aniline compound, 2,6-dimethylaniline, which offers the advantage of reacting through parallel routes (5). It is thus possible to measure directly the hydrogenation and the C–N bond cleavage functions of the catalyst. Moreover, an aniline model molecule is representative of the *o*-propylaniline intermediate in the quinoline reaction network.

Two processes are involved in the hydrodenitrogenation of alkyl anilines: hydrogenation of the aromatic ring and C–N bond cleavage. In the case of hydrogenation of aromatics, with or without an S or N heteroatom, H_2S acts as an inhibitor, but the reaction becomes zero order with respect to H_2S. This response to H_2S has given valuable information about the active species, hydrides and protons, involved in the mechanism of toluene hydrogenation (6). The method has been extended to aromatic sulfur compounds (7, 8). With respect to C–N bond cleavage, the literature distinguishes saturated amines (Csp^3–N) and aromatic amines (Csp^2–N). The former compounds are easily converted into hydrocarbons. Since the reaction is enhanced by H_2S, SH groups are involved in the denitrogenation. Nitrogen removal may proceed by Hofmann elimination after quaternization of the nitrogen atom by a proton. The protonated amine may alternatively undergo an S_N2 nucleophilic substitution by SH^-, followed by the hydrogenolysis of the C–S bond (9–13). In contrast, the reaction of aromatic amines is inhibited by H_2S (5, 14), indicating another mechanism. The direct Csp^2–N bond rupture is still questioned, because of the delocalization of the nitrogen lone pair. An apparent direct heteroatom removal can nevertheless occur through a dihydro intermediate, followed by ammonia elimination, in a way similar to that proposed for the apparent direct desulfurization of dibenzothiophene

[1] To whom correspondence should be addressed. Fax: 33 2 31 45 28 22. E-mail: vangestel@ismra.fr.

0021-9517/01 $35.00
Copyright © 2001 by Academic Press
All rights of reproduction in any form reserved.

(15–17). Nevertheless, Moreau *et al.* (18) showed that, in a series of substituted benzenes, hydride species realize a direct aromatic carbon–N bond cleavage by nucleophilic substitution. This conclusion is based on Hammett correlations and quantum chemical calculations. Jian and Prins (14, 19) suppose a direct hydrogenolysis of the Csp^2–N bond. They report a negative effect of nickel on this reaction and conclude that the hydrogenolysis requires highly unsaturated molybdenum atoms.

We report here a study of the reaction pathways in the hydrodenitrogenation of 2,6-dimethylaniline on a series of cobalt-promoted Mo/Al_2O_3 sulfide catalysts, and two NiMo catalysts. Our aim is to elucidate the reaction mechanism, especially with respect to the Csp^2–N bond cleavage, and to propose a configuration for the active sites. These sites are characterized by IR spectroscopy of adsorbed carbon monoxide, a proven and powerful probe to describe sulfide catalysts (20–22).

EXPERIMENTAL

Catalyst Preparation

The Mo/Al_2O_3 catalyst (8.7 wt% Mo) was prepared by pore-filling impregnation of a γ-alumina support (258 m^2/g, 0.66 cm^3/g) with an ammonium heptamolybdate solution. The sample was dried at 393 K overnight and calcined at 773 K for 3 h. The series of CoMo catalysts were prepared by impregnation of the molybdenum catalyst with a cobalt nitrate solution, drying, and finally calcining at 773 K for 3 h. The catalysts contained 0.1, 1.7, 3.2, and 4.7 wt% cobalt as determined by elemental analyses performed at the Service Central d'Analyse (CNRS, Vernaison). Two $NiMo/Al_2O_3$ catalysts with 0.5 and 1.5 wt% nickel were prepared by impregnation with a nickel nitrate solution, using the same Mo/Al_2O_3 base sample.

2,6-Dimethylaniline Activity Measurement

The reactor (stainless steel reactor system from Sotelem, $L = 300$ mm, i.d. $= 9$ mm) was loaded with 0.25–0.40 g of catalyst grains (0.2–0.5 mm) and pressurized at 4 MPa. The sample was first dried overnight *in situ* at 423 K under N_2 (30 ml/min), and the temperature was decreased to 298 K. Sulfidation was carried out in flowing 10% H_2S/H_2 (30 ml/min) at 623 K for 2 h with a temperature ramp of 3 K/min. Thereafter, the catalyst was cooled under H_2S/H_2 to the reaction temperature of 573 K, and the H_2S content was adjusted at 56 kPa ($H_2S/H_2 = 1.4\%$). The liquid feed (10 vol% 2,6-dimethylaniline, reactant; 80% heptane, solvent; and 10% decane as internal standard) was introduced by an HPLC pump and vaporized in the H_2S/H_2 stream. The reaction products were condensed at the reactor exit and the liquid was analyzed on a gas chromatograph equipped with a CPSIL-5CB capillary column and a FID detector.

The partial pressure of 2,6-dimethylaniline (DMA) was kept constant at 13 kPa for all experiments. Reaction conditions at steady state were varied by changing the contact time (55–250 h · g/mol) at a fixed H_2S partial pressure. Thereafter, the H_2S partial pressure (0–56 kPa) was varied at a fixed contact time. Conversions of DMA were kept below 20%.

FT-IR Spectroscopy of Adsorbed CO

The catalyst powder was pressed into a self-supported wafer (~10 mg, 2 cm^2) and placed into the IR cell. Prior to sulfidation, the catalyst was dried *in situ* at atmospheric pressure at 423 K under N_2, and cooled to 298 K. The catalyst was then sulfided with 10% H_2S/H_2 (30 ml/min) at a rate of 3 K/min up to 623 K. After 2 h of sulfiding, the catalyst was flushed with N_2 for 0.25 h and the temperature was decreased to 298 K. The sulfided catalyst was rapidly evacuated at 573 K (10 K/min) and finally cooled to 100 K for CO adsorption. The catalyst was contacted with 133 Pa CO at equilibrium. IR spectra of adsorbed CO were recorded with a Nicolet Magna 550 IR spectrometer equipped with a MCT detector. For comparison, spectra were normalized to a disc of 10 mg.

Alternatively, after the sulfidation of the catalyst at 623 K, the nitrogen flush was followed by a hydrogen treatment (30 ml/min) at 573 K for 2 h. The catalyst was then cooled under N_2. CO adsorption was performed at 100 K as described above. The two activation procedures are called respectively "sulfided" and "H_2-treated."

RESULTS AND DISCUSSION

Reaction Network of 2,6-Dimethylaniline (DMA)

Figure 1 shows the typical product distribution obtained on the $Co(3.2\%)Mo/Al_2O_3$ catalyst in the presence of 56 kPa H_2S at various contact times. Dimethylcyclohexenes (DMCHe) and dimethylcyclohexanes (DMCHa) are lumped and are the major denitrogenation products. The other denitrogenation product is *m*-xylene (Xyl), formed in small quantity. We checked that under our conditions, *m*-xylene is not hydrogenated. Finally, large quantities of 2-methylaniline and 2,4,6-trimethylaniline are observed, in approximately equal amounts. These products result from the disproportionation (DIS) of DMA. All three groups of products appear to be primary products. We determined the reaction orders for the formation of DMCHe + DMCHa (k_1), Xyl (k_2), and DIS (k_3') as zero, zero, and 0.4, respectively. Previously we reported first-order kinetics (5). The difference is due to the DMA partial pressure, 13 kPa instead of 1.3 kPa. Activities are expressed by the rate constants. For the sake of uniformity of units, the activity for DIS is given by $k_3 = k_3'(P^\circ_{DMA})^{0.4}$ mol · h^{-1} kg^{-1}.

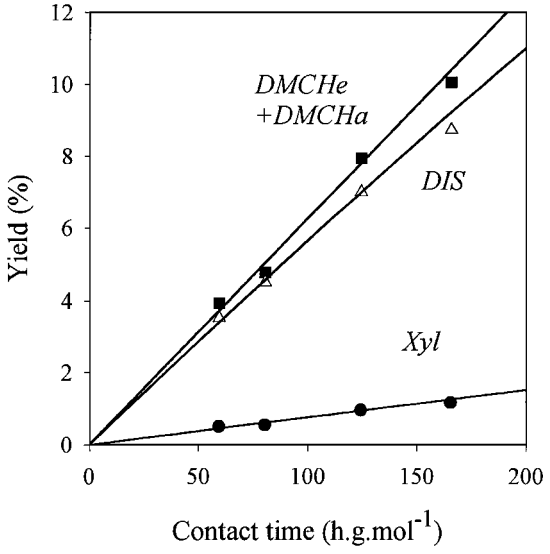

FIG. 1. Product distribution for the reaction of 2,6-dimethylaniline at 573 K in the presence of 56 kPa H_2S on the Co(3.2%)Mo/Al_2O_3 catalyst.

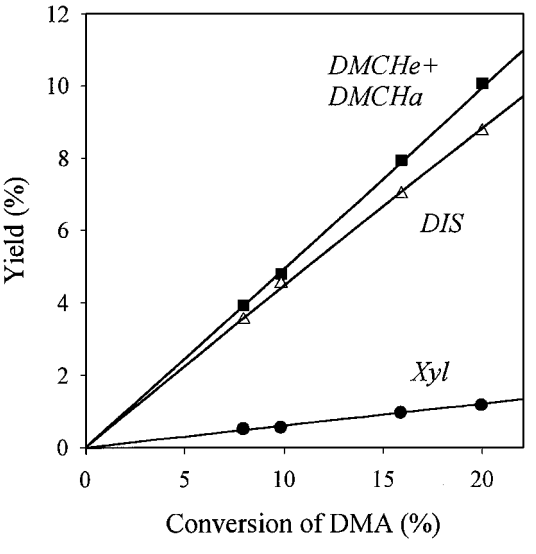

FIG. 2. Selectivity diagram for the reaction of 2,6-dimethylaniline in the presence of 56 kPa H_2S on the Co(3.2%)Mo/Al_2O_3 catalyst.

The selectivity diagram (Fig. 2) shows that the three routes run strictly parallel up to 20% conversion of DMA. The selectivity for xylene does not exceed 5% of total conversion, including the disproportionation of DMA, and 12% if only the denitrogenated products are taken into account. These results compare well with those reported for other Co(Ni)Mo/Al_2O_3 catalysts measured at much lower DMA pressure (5). They contrast with those reported by Moreau *et al.* (23) for the HDN of aniline in a batch reactor at 613 K and 7 MPa, yielding 80% selectivity for benzene over a CoMo catalyst in the absence of H_2S. Over a NiMo catalyst, under the same conditions, the hydrogenation route was predominant (23). Pérot *et al.* (24) reported a high selectivity for hydrogenation products in the study of 2,6-diethylaniline in a flow reactor at 623 K and 7 MP a over NiMo catalysts in the presence of H_2S. More recently, Rota and Prins (11) reported also a high selectivity in hydrogenation products (95%) in the conversion of *o*-toluidine over NiMo catalysts. None of these studies mentioned the disproportionation route in the product distribution.

With the exception of the disproportionation, all the studies agree with the general HDN reaction scheme for aniline type compounds with two parallel routes: hydrogenation and apparent direct nitrogen removal. This looks very similar to the generally accepted scheme for the hydrodesulfurization of dibenzothiophene (16). Accordingly, these parallel denitrogenation routes most probably proceed through a preliminary dearomatization step yielding a dihydro intermediate. The proposed reaction network for DMA is depicted in Scheme 1.

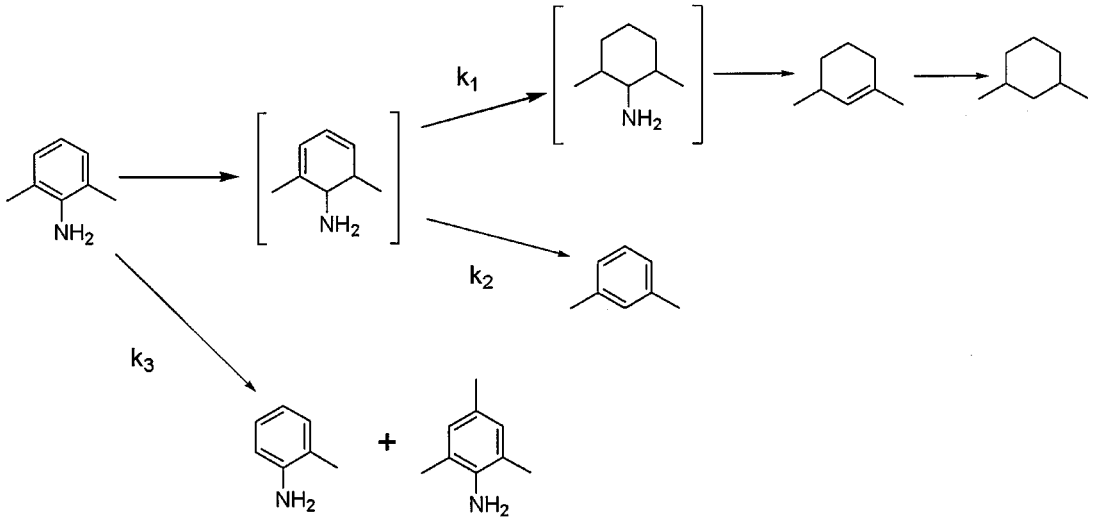

SCHEME 1. Reaction network of 2,6-dimethylaniline.

In this scheme, dimethylcyclohexenes and dimethylcyclohexanes are formed through a complete hydrogenation of the dihydro intermediate into dimethylcyclohexylamine, followed by a fast elimination of ammonia. Alternatively, the dihydro intermediate may undergo elimination of ammonia, yielding xylene and thus restoring the aromaticity. Eventually, as proposed by Rota and Prins (11), substitution of the amino group on the dihydro or hexahydro intermediates by SH may precede elimination of the heteroatom. However, such thiol intermediates are not detected under our conditions. The limiting step for both routes should be dearomatization, because we did not observe any intermediate. The selectivity is governed by the relative rate constants k_1 and k_2 and adsorption coefficients. Disproportionation does not contribute to nitrogen removal unless the isomerized methylanilines follow a scheme similar to that of DMA. Only traces of monomethyl and trimethyl HDN products were detected.

Influence of H_2S

Figure 3 shows the influence of H_2S partial pressure on the three routes over the Co(3.2%)Mo/Al_2O_3 catalyst. The rate constants k_1 and k_2 abruptly decrease with minute amounts of H_2S (up to 300 ppm), and exhibit zero order with respect to H_2S. It is worth mentioning that the effect of H_2S partial pressure on the reaction of DMA is totally reversible. The disproportionation route (k_3) increases with increasing H_2S pressure and is not occurring on the bare alumina carrier. It follows almost a half-order dependency in H_2S, implying that dissociated H_2S is involved in the reaction mechanism. H_2S is indeed known to create Brønsted acidity over sulfide catalysts, located on the sulfide phase

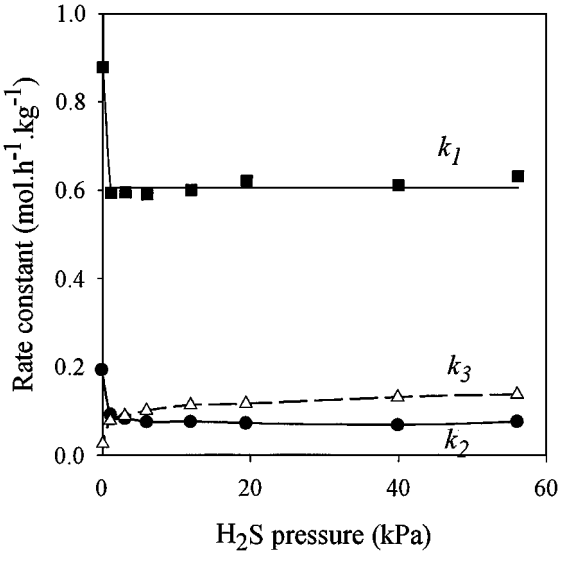

FIG. 3. Influence of H_2S on the activity of the Co(3.2%)Mo/Al_2O_3 catalyst for the three reaction routes: k_1, formation of dimethylcyclohexenes and -anes; k_2, formation of *m*-xylene; k_3, disproportionation.

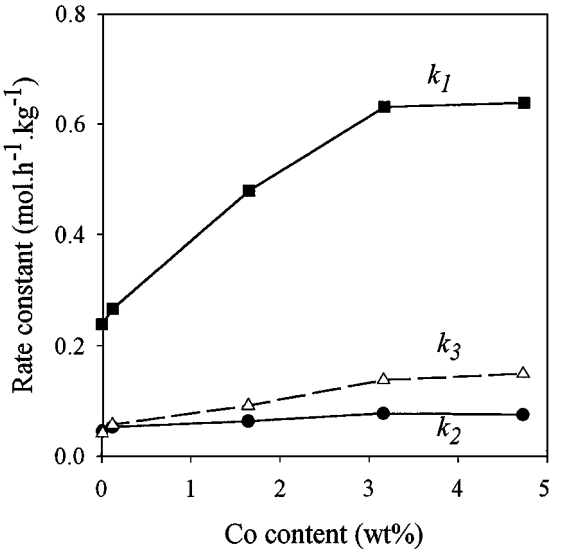

FIG. 4. Influence of cobalt content on the rate constants for DMCHe + DMCHa (k_1), Xyl (k_2), and DIS (k_3) in the presence of 56 kPa H_2S.

and on the alumina carrier (25–27). Because H_2S accelerates DIS, we are inclined to suggest an acidic mechanism occurring on the sulfide phase and/or on alumina.

With respect to k_1 and k_2, the abrupt inhibition by H_2S followed by a stabilization looks very similar to the H_2S sensitivity reported for aromatic hydrocarbons hydrogenation (6). It contrasts with the continuous decrease in activity for hydrodesulfurization of model sulfur-containing molecules (28). This different behavior can be attributed to the relative equilibrium adsorption constants, much larger for H_2S than for DMA, but comparable for H_2S and organic sulfur compounds. Although not the purpose of this paper, it is worth mentioning that the zero order in H_2S has drawn particular attention in literature. Two main models interpreting the change in reaction order with H_2S pressure emerge from kinetic studies. Kasztelan and Guillaume (6) proposed a change in the rate-determining step in the sequence of elementary reactions for toluene hydrogenation: first addition of H^- or H^+ to the aromatic ring. Olguin-Orozco and Vrinat (7) extended this model to dibenzothiophene. Alternatively, we proposed a gradual conversion of vacancy sites into sulfur-saturated sites (2). However, under high hydrogen pressure, the kinetics cannot discriminate between the two models, both of them satisfactorily explaining the zero order in H_2S.

Influence of Cobalt Content in the Presence of H_2S

The reactivity of DMA over the series of Co(0–4.7%)Mo/Al_2O_3 samples was studied in the range of 0–56 kPa H_2S partial pressure. Since nitrogen removal is zero order in H_2S, only data for 56 kPa H_2S are reported here. Figure 4 shows the influence of the cobalt content on the

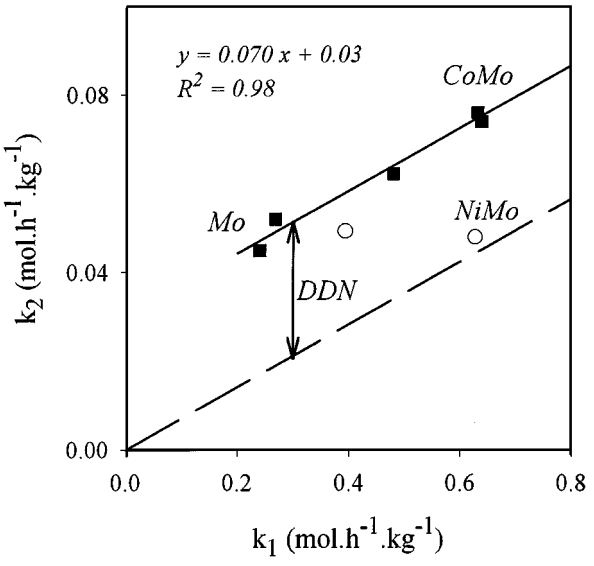

FIG. 5. Rate constant for xylene formation (k_2) as a function of DMCHe + DMCHa formation (k_1) for the reaction performed in the presence of 56 kPa H_2S over the series of Co(0–4.7%)Mo/Al_2O_3 catalysts (■) and two NiMo/Al_2O_3 catalysts (0.5 and 1.5% Ni, ◯).

rate constants measured in the presence of H_2S. Clearly, all three routes are promoted by cobalt, including disproportionation. The activity is leveling off for Co contents above about 3 wt%. Thus, the maximum of promotion is obtained for a Co/Co + Mo ratio of 0.33, as expected for mixed sulfide catalysts. The rate constant increase for disproportionation is in line with the higher efficiency of the promoted catalyst for dissociation of H_2S (25). Thus, the concentration of acidic sites induced by H_2S is increased by cobalt, which leads to a higher activity for the disproportionation on the promoted catalyst. For the two other routes, the activity enhancement is more important for hydrogenation (promotion factor of 2.6) than for elimination (factor 1.7). Different promotion factors were also observed in the case of dibenzothiophene, the direct desulfurization route being much more sensitive to the promoter than the hydrogenation route (17, 29). The authors explained the difference in the promotion factors by a change in the rate-limiting step: C–S bond cleavage for the Mo catalyst against dearomatization for the CoMo catalyst. With DMA, if (Fig. 5) the rate constant for xylene formation (k_2) is plotted against the rate constant for the formation of DMCHe + DMCHa (k_1), we obtain a straight line. Addition of cobalt thus increases both k_2 and k_1 in a constant ratio $\Delta k_2/\Delta k_1 = 0.070$. This linear relationship can be interpreted in different ways.

First, if xylene is only the result of a direct cleavage of the aromatic C–N bond, independently of hydrogenation, the linear relationship simply means that the promoted sites have a better ability to catalyze both hydrogenolysis and hydrogenation than the unpromoted Mo catalyst. However, our results obtained without H_2S, described in the following section, show clearly a negative effect of cobalt on the rate constant k_2 for xylene formation. We think that it is unlikely that this hydrogenolysis would be promoted in the presence of H_2S, while inhibited in the absence of H_2S. For the hydrogenation route, such a change is not observed: promotion is observed in both cases. Moreover, addition or removal of H_2S in the reaction medium is completely reversible and the intermediate region (between 0 and 300 ppm of H_2S) shows a continuous change in selectivity.

Second, one can propose that the *m*-xylene is formed uniquely in parallel to the DMCHe + DMCHa products, after dearomatization. In that case, cobalt addition promotes the dearomatization step, yielding the common dihydro intermediate. The heteroatom removal occurs by a Csp^3–N bond cleavage (elimination) from the dihydro intermediate, much easier than the cleavage of the aromatic Csp^2–N bond. However, the absolute selectivity k_2/k_1, quantified by the slope of the straight line, should be constant, whatever the cobalt content, and the extrapolated line should go through the origin.

We believe therefore that the linear relationship in Fig. 5 corresponds to a combination of the two mechanisms. Xylene is partly formed after dearomatization, with a constant selectivity hydrogenation/elimination. This route is effectively promoted by cobalt. The *Y* intercept shows that dearomatization is not the only way to produce *m*-xylene. The dearomatization route is represented in Fig. 5 by the dashed line, going through the origin, and parallel to the experimental line. The difference with the experimental line corresponds to a constant formation of xylene in the presence of H_2S, amounting to 0.03 $mol \cdot h^{-1} \cdot kg^{-1}$, and independent of the cobalt content of the catalysts. A portion of the observed xylene then comes directly from the DMA molecule, without any preliminary dearomatization. The corresponding reaction network is represented in Scheme 2. Direct aromatic carbon–nitrogen bond cleavage may occur by hydrogenolysis or by hydride substitution as discussed later. Under our conditions, in the presence of H_2S, the contribution of this direct denitrogenation (DDN) route to the total xylene formation is rather important since it amounts to about 65% on the Mo catalyst and 40% on

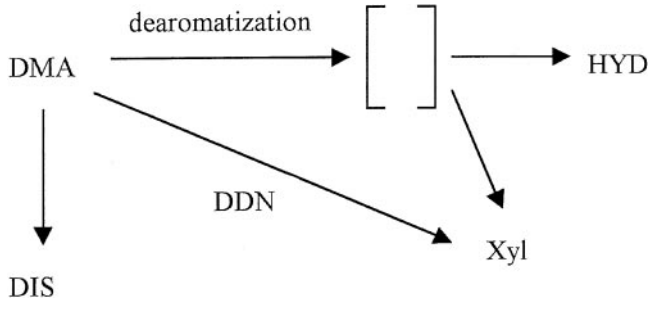

SCHEME 2. Improved reaction network for the HDN of 2,6-dimethylaniline.

the Co(3.2%)Mo catalyst. This DDN activity is independent of cobalt content, and we conclude that it proceeds on Mo sites distinct from those involved in dearomatization. Moreover, these typical Mo sites are not influenced by Co promotion. This will be discussed in view of the decoration model in the Mechanism and Catalytic Sites section.

One may argue that the k_2–k_1 relationship reported in Fig. 5 for the CoMo catalysts is not general for mixed sulfide catalysts. In particular, the NiMo couple is known to present a hydrogenolysis–hydrogenation selectivity different from that of CoMo, and thus will not follow the same line as for the CoMo catalysts in Fig. 5. Although it is not the aim of this paper, focusing on CoMo catalysts, we measured the activity of two NiMo samples with a nickel content below the full promotion level. The corresponding data are plotted in Fig. 5. The rate constant for xylene formation, k_2, is fairly constant and very close to that measured for the unpromoted Mo catalyst; the rate constant k_1 for the hydrogenation route increases with increasing Ni content. This may be interpreted as in the case of the CoMo catalysts. Nickel promotes both k_1 and k_2 via dearomatization through a common intermediate. However, the selectivity factor $\Delta k_2/\Delta k_1$ might be lower for NiMo than for CoMo, due to its known hydrogenation properties. In that case, dearomatization should be represented by a dashed line going through the origin, but with a lower slope than for the CoMo catalysts. However, the difference between the observed k_2 and the xylene formed after dearomatization, representing the DDN reaction, is not constant for the NiMo catalysts; it diminishes continuously with increasing Ni content. The constant xylene formation measured is thus the result of the compensating effect between the promoted dearomatization route and the inhibited DDN pathway. This means that the specific Mo sites responsible for the direct formation of xylene, found to be insensitive to cobalt, are poisoned in the case of the nickel promoter.

The surface sites on the "sulfided" CoMo catalysts were characterized by infrared spectroscopy of adsorbed CO. We performed CO adsorption at 100 K, in order to increase the coverage of the probe molecule on weak sites such as those present on the unpromoted Mo phase. Under these conditions, the IR spectra show the interaction of the probe with the alumina carrier and with the sulfide phase (21, 22). Results obtained on the series of sulfided CoMo catalysts are presented in Fig. 6. For all samples, CO adsorbs on the coordinated unsaturated (CUS) Al^{3+} sites (band at around 2190 cm^{-1}) and interacts with the hydroxyl groups of the alumina carrier (band at 2154 cm^{-1}). The sulfide phase is characterized by a band at 2110 cm^{-1} assigned to the CUS located on molybdenum and by a signal at 2070 cm^{-1} for the promoted sites (20). The variation of the band intensities with cobalt content confirms such an assignment, since the number of promoted sites increases at the expense of

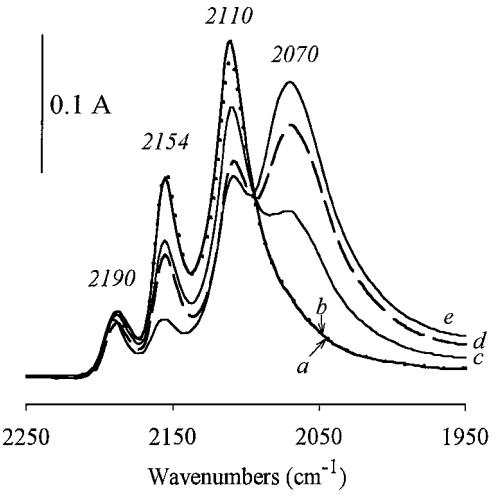

FIG. 6. FT-IR spectra of CO adsorbed at 100 K on "sulfided" Mo and CoMo catalysts: (a) Mo (solid line); (b) Co(0.1%)Mo (dotted); (c) Co(1.7%)Mo (solid); (d) Co(3.2%)Mo (dashed); (e) Co(4.7%) Mo/Al_2O_3 (solid).

unpromoted Mo sites. However, a fraction of unpromoted sites still remains, even for the Co(4.7%)Mo catalyst, beyond the composition for maximum global activity. The signal at 2070 cm^{-1} appears to increase between 3.2 and 4.7% Co. This may be due to a contribution of adsorbed CO on excess cobalt. However, no signal at 2055 cm^{-1} for adsorption on cobalt sulfide, not involved in promotion, is detected in our series of catalysts. Cobalt addition also leads to an intensity decrease of the bands characterizing the carrier, in particular these specific to acidic OH groups. This is indicative of a decrease of the support acidity by cobalt spinel formation.

With the exception of the sample with excess cobalt, the intensity of the bands specific to the unpromoted and promoted sites of the sulfide phase follows the denitrogenation ($k_1 + k_2$) activity of DMA, as shown by the linear correlation in Fig. 7. This activity includes the extra xylene formation by DDN, but this will not affect the correlation, since the DDN activity is minor and constant for the CoMo series (Fig. 5). This correlation means that the dearomatization activity is a linear combination of the intrinsic activities of unpromoted and promoted sites (30).

With respect to the sites responsible for the DDN pathway, the spectra of the sulfided catalysts do not show a specific signal of the sulfide phase accounting for the extra xylene formation. This is attributed to a very low concentration of sites, as indicated by the low DDN activity measured in the presence of H_2S.

Influence of Cobalt Content in the Absence of H_2S

In the absence of H_2S, cobalt influences the three routes, i.e., hydrogenation, xylene formation, and disproportionation, differently. The rate constants are plotted as a function

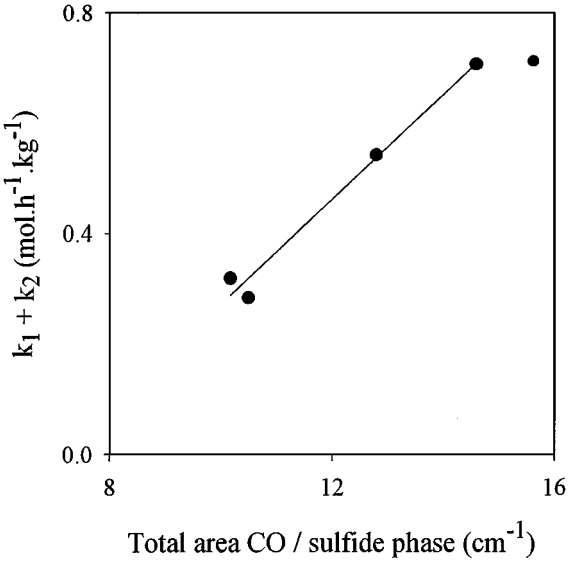

FIG. 7. Relationship between dearomatization activity ($k_1 + k_2$) and the total intensity of the signal of adsorbed CO on the sulfide phase for the series of Co(0–4.7%)Mo/Al_2O_3 catalysts.

of Co content in Fig. 8. DIS (k_3) is considerably lowered, and slightly promoted by cobalt. The hydrogenation route, k_1, is highly promoted by cobalt, as was the case in the presence of H_2S. The striking result concerns xylene formation, k_2, for which cobalt exhibits a marked negative effect. Such a negative promoter effect was already reported by Jian and Prins (19) in the case of *o*-propylaniline over Mo and NiMo catalysts. As a result, the xylene selectivity depends strongly on Co content. Without H_2S, the Mo catalyst is very selective toward xylene (60% of the denitrogenated products), while the selectivity remains low (18%) on the Co(3.2%)Mo catalyst. The selectivity inversion indicates that the parallel between k_1 and k_2, which was established in the presence of H_2S, is not observed anymore. It is a strong indication that there is an extra xylene formation, more pronounced for low cobalt content catalysts. Most probably, the DDN route, revealed in the presence of H_2S, is more important without H_2S.

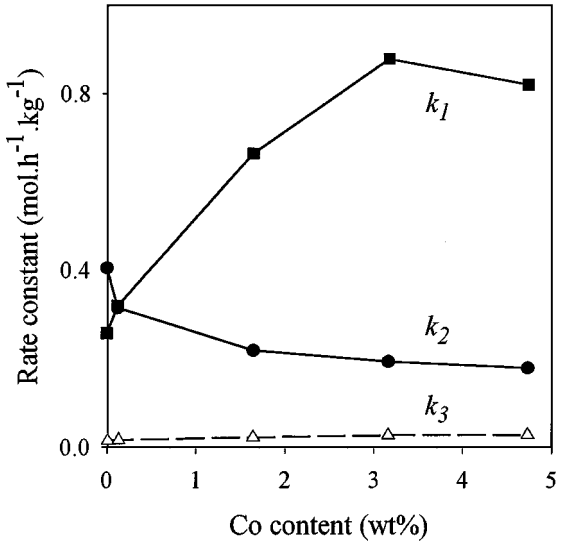

FIG. 8. Influence of cobalt content on the rate constants for DMCHe + DMCHa (k_1), Xyl (k_2), and DIS (k_3) for the reaction of DMA performed in the absence of H_2S.

To quantify the evolution of the DDN route with cobalt content, we still consider that a fraction of the total xylene is formed after dearomatization by a route strictly parallel to hydrogenation. However, without H_2S, the selectivity factor $\Delta k_2/\Delta k_1$ is unknown. We assume a value of 0.070, as found in the presence of 56 kPa of H_2S (Fig. 5). From k_1, we can calculate $k_{2\text{dearo}}$ for each catalyst, representing the activity for xylene formation via dearomatization. The difference with the measured rate constant k_2 for xylene formation gives the DDN activity $k_{2\text{DDN}}$. The values in Table 1 show that the contribution of DDN to total xylene formation is very important on the Mo catalyst (0.39 mol · h^{-1} · kg^{-1}) and decreases with increasing cobalt content to a level of 0.12 mol · h^{-1} · kg^{-1}. This clearly evidences a reversed promoting effect, a so-called "demoting effect," of cobalt on direct aromatic carbon–nitrogen bond cleavage. We recall that in the presence of H_2S, this DDN activity is low and constant (0.03 mol · h^{-1} · kg^{-1}). This means that specific "DDN" sites are created in much larger amounts in the absence of H_2S, especially on the Mo catalyst. The negative effect of cobalt confirms that these DDN sites are located on molybdenum only.

Such drastic changes in activity and selectivity observed without H_2S could alternatively result from a modification of both the structure and the number of surface sites, upon contact with large amounts of hydrogen at high temperature. To answer this question, we carried out CO adsorption after a mild H_2 treatment (573 K) of the sulfided catalyst in order to mimic the reaction atmosphere as closely as possible. These activation conditions considerably modify the CO spectra. As an example, the spectrum of the "H_2-treated" unpromoted Mo catalyst in Fig. 9 shows a

TABLE 1

Calculated Activities for the DDN Route in the Absence of H_2S

	Rate constant (mol · h^{-1} · kg^{-1})		
Co content (wt%)	k_1	k_2	$k_{2\text{DDN}}$
0	0.26	0.41	0.39
0.1	0.32	0.32	0.29
1.7	0.66	0.22	0.17
3.2	0.88	0.19	0.13
4.7	0.82	0.18	0.12

2-fold increase in the amount of Mo CUS as compared to the "sulfided" sample, indicating that the removal of sulfur by hydrogen has created vacancies, as expected (31, 32). An interesting feature in the spectrum is the appearance of a shoulder (2098 cm^{-1}) at a lower wavenumber than usually observed for Mo vacancy sites (2110 cm^{-1}). This new band at 2098 cm^{-1} is better evidenced by subtracting the spectra of CO adsorbed on the "H_2-treated" catalysts and on the "sulfided". We have verified that the original signal of the "sulfided" catalyst is restored after contacting the "H_2-treated" catalyst with $H_2S(10\%)/H_2$ at 573 K. Hence, the structure of the MoS_2 slab has been preserved and only labile sulfur has been removed. In a recent work, Travert *et al.* (32) suggested, on the basis of density functional theory calculations, a lower sulfur coordination of the site corresponding to the band at around 2095 cm^{-1} than on the site corresponding to the ν(CO) at 2110 cm^{-1}. It is worth mentioning that the activation conditions of the "H_2-treated" catalysts are very favorable for the observation of a maximum of CUS and in particular for the detection of the ν(CO) band at 2098 cm^{-1}. Indeed, catalysts were treated successively under a flow of H_2S/H_2 and of H_2. Both sulfidation and H_2 treatment steps were followed by flushing under inert gas at high temperature to avoid adsorption of H_2S or contaminants like COS (always present as impurity in H_2S) or H_2O. This might be the reason why previous studies did not report the presence of the band at 2098 cm^{-1} (31). Activation conducted under static conditions gives a broad shoulder at 2100–2095 cm^{-1} of much lower intensity, which is difficult to observe (32). The hydrogen treatment also leads to a strong increase of the number of CUS of the sulfided phase for the series of CoMo catalysts (spectra not presented). The difference spectra between "H_2-treated" and "sulfided" catalysts

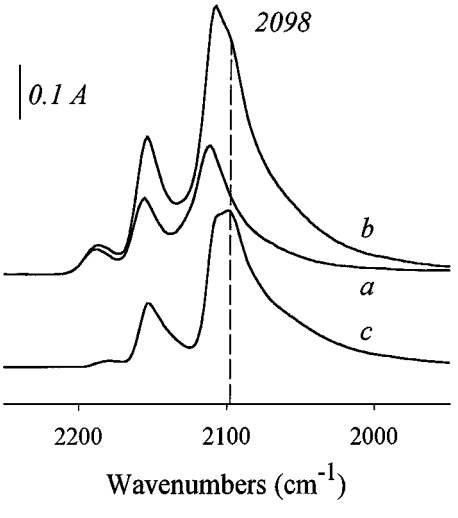

FIG. 9. FT-IR spectra of CO adsorbed on "sulfided" (a) and "H_2-treated" (b) Mo/Al_2O_3 catalysts. (c) Difference (b) − (a).

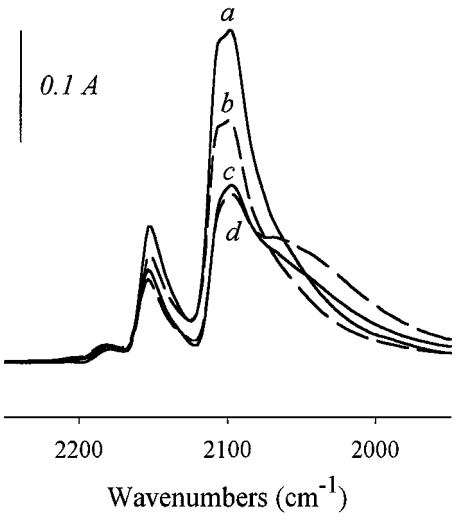

FIG. 10. Difference spectra "H_2-treated" − "sulfided" for the CoMo series: (a) Mo (solid line); (b) Co(0.1%)Mo (dashed); (c) Co(1.7%)Mo (solid); (d) $Co(3.2\%)Mo/Al_2O_3$ (dashed).

of the CoMo samples, representative of the promoting effect, are shown in Fig. 10. The band intensities highlight a marked increase of the number of unpromoted sites rather than promoted sites. This is even accentuated by the larger molar extinction coefficient of the CO band characteristic of the promoted sites (21). The intensity of the band at 2070 cm^{-1} increases moderately, only upon H_2 treatment on catalysts containing the highest cobalt content (1.7 and 3.2%). It is attributed to an increased number of promoted sites rather than to the creation of unpromoted sites in a specific environment. The number of promoted sites created by H_2 posttreatment increases more strongly above 1.7% cobalt content, and accounts for the increased dearomatization activity without H_2S. On all the catalysts of the series, the new band at 2098 cm^{-1} is created upon H_2 treatment and, as observed in Fig. 10, the ratio between the number of sites characterized by the bands at 2110 and 2098 cm^{-1} is constant whatever the catalyst. The intensity of these two bands is by far the most important for the Mo catalyst; it diminishes rapidly with cobalt content, and almost stabilizes at 1.7% cobalt. The similarity between the intensity of the band at 2098 cm^{-1} and the decrease of the DDN activity with cobalt in the absence of H_2S (Table 1) is striking. It strongly indicates that these Mo sites are involved in the aromatic C–N bond rupture.

Mechanism and Catalytic Sites

In this section, we propose a mechanism, essentially for the heteroatom removal. On one hand, dearomatization followed by further elimination and hydrogenation, and on the other hand, direct aromatic carbon–nitrogen bond cleavage. However, the disproportionation reaction also deserves some attention. Indeed, the reaction is unusual on

sulfides, and yields substantial amounts of products under our conditions.

Disproportionation reactions are typically acid-catalyzed, and have been well documented, for example in the case of xylene production from toluene on acidic zeolites (33). On sulfide catalysts, the acidity is too low to provoke such a reaction, and the formation of 2-methylaniline and 2,4,6-trimethylaniline from DMA must occur somewhat differently. Necessarily, the transition state for this reaction should present the bonding of one DMA molecule through a methyl group to the para position of the other DMA (Scheme 3). Our results indicate that acidity brought by H_2S dissociation is clearly involved. Therefore, we may suggest a protonation of the amino group of the DMA molecule. The two methyl substituents in 2 and 6 positions favor this protonation. Consequently, the methyl groups become positively charged. The effect may be reinforced by adsorption of the C_3 or C_5 carbon atoms. The positively charged methyl group may then bind to the para position of a DMA molecule in the gas phase or physisorbed on the catalyst. This intermediate may then easily split into the observed disproportionation products.

The routes for nitrogen removal are very much like the hydrodesulfurization of dibenzothiophene (17). The adsorption site for dearomatization (hydrogenation) is a promoted or unpromoted Mo atom with one or several vacancies. Its degree of unsaturation is not necessarily as high as that proposed by the authors of Ref. (17), because DMA dearomatization is not very sensitive to H_2S. The active species for dearomatization (hydrogenation) are generated by hydrogen dissociation, yielding a hydride on an anionic vacancy, and a proton associated with a neighboring S^{2-}. The rate-limiting step is addition either of a hydride ion (6, 7) or of a proton (2, 5, 8). With respect to elimination, the required basic site involved in the E_2 mechanism is provided by S^{2-} on the edges of the MoS_2 slabs (29). In the absence of H_2S, the concentration of vacancies is increased, as is the activity for dearomatization.

The difference between the DMA and dibenzothiophene behavior is the evidence for direct heteroatom removal (DDN) without preliminary dearomatization of the DMA molecule. This particular reaction is of importance over the unpromoted Mo catalyst, in the absence of H_2S. The DDN activity is readily poisoned by H_2S and, surprisingly, it decreases with the cobalt content of the catalyst. This means that the reaction requires a specific configuration of sites located exclusively on Mo, with a high degree of unsaturation (14).

The reaction can proceed either by hydrogenolysis or by nucleophilic substitution by hydride. Although the former mechanism cannot be ruled out, the latter one is strongly supported by the recent work of Moreau *et al.* (18). Studying the carbon–heteroatom bond cleavage of a series of substituted benzenes over unsupported transition metal sulfides, they conclude from Hammett correlations and quantum chemical modeling that a nucleophilic substitution by hydrides takes place. Hydrides formed by dissociation of hydrogen can react in two ways: nucleophilic substitution leading to the DDN route, or following Kasztelan and Guillaume (6), addition to the aromatic ring as the first step for dearomatization. Since we observe a predominance of DDN on the Mo catalyst, especially in the absence of H_2S, dearomatization is not favored. Probably, there is a lack of protons in the near vicinity of the adsorbed molecule to complete the formation of the dihydro intermediate. Indeed, protons are attached to a sulfur atom and can migrate only if a host sulfur is available in proximity. This situation does not occur in the configuration depicted in Scheme 4 for the unpromoted Mo catalyst in the absence of H_2S. Moreover, in order to favor the nucleophilic substitution in the DDN process, the aromaticity of the molecule should be destabilized. This can be achieved by simultaneous adsorption of the nitrogen atom and the aromatic ring on two adjacent vacancies. Additionally, hydrogen dissociation requires a bridging sulfur atom and a vacancy, which are converted into a SH group and a hydride adsorbed on the Mo atom. The hydride attack on the Csp^2 carbon cannot be followed by proton addition due to the distance between the SH group and the Mo with a high degree of unsaturation, thus excluding hydrogenation. Finally, NH_3 is evolved by hydrogen, which regenerates the original adsorption site.

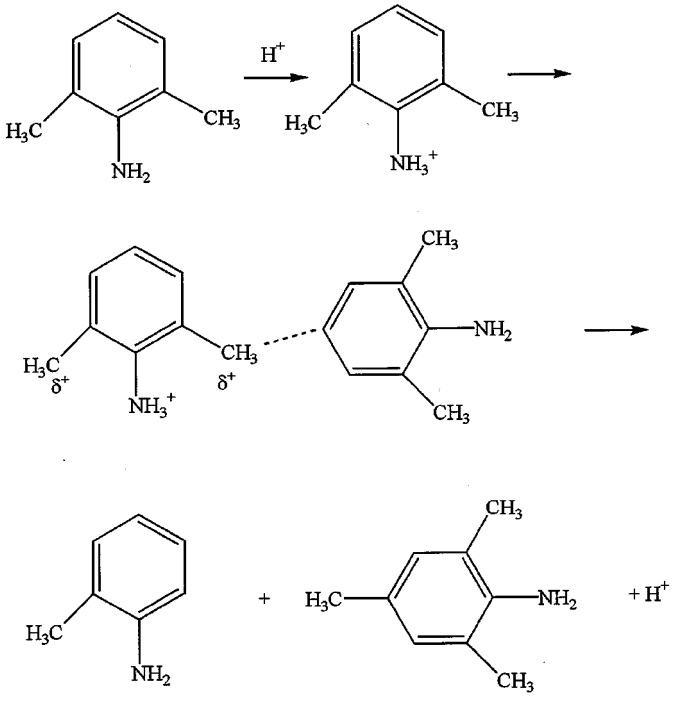

SCHEME 3. Mechanism for the disproportionation of 2,6-dimethylaniline.

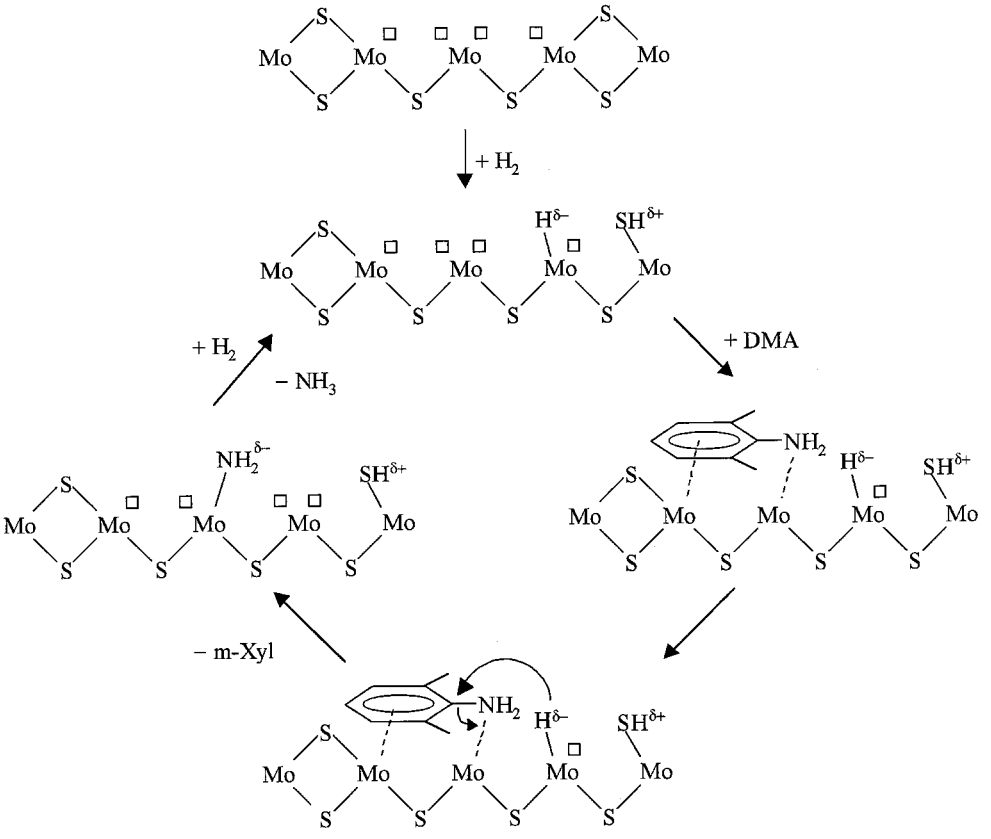

SCHEME 4. Proposed active sites and reaction mechanism for the direct denitrogenation (DDN) in the absence of H_2S.

Therefore, all these features indicate that the crucial requirement for the DDN pathway is the presence of at least three adjacent Mo sites with one Mo atom highly depleted in sulfur. This configuration may well account for the IR signal detected on the unpromoted phase after H_2 posttreatment. Indeed, the bands at 2110 and 2098 cm^{-1} reveal the presence of two Mo sites in a close but somewhat different environment, likely Mo sites situated on the same edge of the MoS_2 slab, the band at 2098 cm^{-1} characterizing Mo sites with a lower sulfur coordination. Taking into account *ab initio* calculations (32), it was proposed that these sites are situated on the Mo edge of the MoS_2 crystallites. The configuration depicted in Scheme 4 may account for the specificity of the sites required for DDN. Nevertheless, we cannot exclude that some active sites are also situated on the sulfur edge. Indeed, on the Mo catalyst, H_2 treatment leads also to the appearance of a weak shoulder at 2070 cm^{-1} which, taking into account the previous work of Travert *et al.* (32), characterizes highly unsaturated Mo on the sulfur edge. We should also keep in mind that the H_2 treatment is performed under atmospheric pressure in the IR cell, while the pressure reaches 4 MPa under the reaction conditions. The specific activity of sites presenting a higher degree of unsaturation has already been proposed (14).

The observed negative effect of cobalt on the DDN activity without H_2S may be interpreted by a strong limitation of the probability to create the arrangement of several adjacent Mo vacancies. If so, vacancies associated with cobalt in the CoMo catalyst are not equivalent to vacancies on pure Mo. Indeed, CO adsorption provides evidence for a modification of the electronic properties of the site when promoted. We can propose that these electronic properties are unfavorable for the multipoint adsorption of the aniline necessary for the DDN route. Even at 3.2 wt% Co, corresponding to a full promotion with respect to the global activity, the DDN activity without H_2S is not completely inhibited by Co. It remains at a level of 0.12 $mol \cdot h^{-1} \cdot kg^{-1}$, which is 4 times higher than the activity in the presence of H_2S. This means that a part of the slab cannot be promoted, which is in agreement with the observations by IR spectroscopy of adsorbed CO. We can propose that promotion by Co occurs only on one of the exposed edges of the MoS_2 slab, either the (1010)S-edge or the (1010)Mo-edge. Based on this reactivity study, we cannot distinguish between these edges, but a recent scanning tunneling microscopy study indicated a preferential decoration of the S-edge of the MoS_2 slab (34).

The DDN reaction needs a highly unsaturated configuration located on Mo atoms as depicted in Scheme 4. These

sites are expected to be very sensitive to H_2S. Indeed, on the unpromoted Mo catalyst, the high DDN activity in the absence of H_2S diminishes readily after addition of H_2S in the reactor, the highly unsaturated edge sites being easily poisoned. However, some activity remains on specific sites that are insensitive to H_2S, for which corner sites can be proposed. Running the promoted CoMo catalysts in the presence of H_2S yields a low DDN activity on these specific sites, which can never be promoted by cobalt.

On nickel-promoted catalysts, the situation is different. Indeed, already in the presence of H_2S, the DDN activity decreases with Ni content. This points out that nickel interacts differently than cobalt with the MoS_2 slabs, and might promote all the edge and corner sites of MoS_2.

CONCLUSION

HDN of 2,6-dimethylaniline shows the parallel formation of three groups of products: (i) dimethylcyclohexenes and dimethylcyclohexanes, (ii) *m*-xylene, and (iii) 2-methylaniline and 2,4,6-trimethylaniline. The isomerized anilines result from disproportionation, promoted by cobalt and by acidity provided by the dissociative adsorption of H_2S.

DMA is dearomatized, and the formed dihydro intermediate reacts in two ways: further hydrogenation to dimethylcyclohexylamine, undergoing a rapid NH_3 elimination, resulting in dimethylcyclohexenes and -anes; or elimination of NH_3 to form *m*-xylene. The common dearomatization step is promoted by cobalt, and inhibited by H_2S.

We highlight a second route for xylene formation, direct denitrogenation (DDN) of the aromatic aniline, occurring by a nucleophilic substitution by a hydride species. The sites responsible for this reaction are located uniquely on highly unsaturated Mo atoms. These sites are detected by FT-IR spectroscopy of adsorbed carbon monoxide after a mild hydrogen treatment of the sulfided catalyst, giving rise to a new band at 2098 cm^{-1}, not observed on the "sulfided" catalyst. The intensity variation of this band correlates with the activity of the catalyst in the absence of H_2S for the direct Csp^2–N bond cleavage.

The DDN pathway, important in the absence of H_2S, is readily inhibited by H_2S. The reaction without H_2S is decreased by addition of cobalt. In the presence of H_2S, the contribution of this DDN route for xylene formation is low, but independent of Co content.

In the case of NiMo catalysts, inhibition by Ni is observed, even in the presence of H_2S. Our results indicate a preferential location of Co on only one type of MoS_2 edges (either S or Mo edge), resulting in an incomplete decoration of the slab. On the other hand, there is no preference for the Ni location. The reaction of DMA is very valuable since it suggests different interactions of Co and Ni as promoters of the MoS_2 slabs. Furthermore, the different catalytic functions measured with DMA, i.e., hydrogenation, direct denitrogenation, and acidity, make this aniline very valuable as a model molecule for sulfide catalysts. For example, one can envisage its use for understanding the hydrogenation of aromatics and hydrodesulfurization of sulfur compounds in gasoil.

REFERENCES

1. Topsøe, H., Clausen, B. S., and Massoth, F. E., *in* "Catalysis, Science and Technology" (J. R. Anderson and M. Boudart, Eds.), Vol. 11. Springer-Verlag, Berlin, 1996.
2. Leglise, J., Finot, L., van Gestel, J. N. M., and Duchet, J. C., *Stud. Surf. Sci. Catal.* **127**, 51 (1999).
3. Ho, T. C., *Catal. Rev.-Sci. Eng.* **30**, 117 (1988).
4. Girgis, M. J., and Gates, B. C., *Ind. Eng. Chem. Res.* **30**, 3021 (1991).
5. Van Gestel, J., Leglise, J., and Duchet, J. C., *Appl. Catal. A* **92**, 143 (1992).
6. Kasztelan, S., and Guillaume, D., *Ind. Eng. Chem. Res.* **33**, 203 (1994).
7. Olguin-Orozco, E., and Vrinat, M., *Appl. Catal. A* **170**, 195 (1998).
8. Van Gestel, J., Finot, L., Leglise, J., and Duchet, J. C., *Bull. Soc. Chim. Belg.* **104**, 189 (1994).
9. Nelson, N., and Levy, R. B., *J. Catal.* **58**, 485 (1979).
10. Cerný, M., *Collect. Czech. Chem. Commun.* **49**, 2387 (1984).
11. Rota, F., and Prins, R., *Topics Catal.* **11/12**, 327 (2000).
12. Pérot, G., *Catal. Today* **10**, 447 (1991).
13. Portefaix, J. L., Cattenot, M., Guerriche, M., Thivolle-Cazat, J., and Breysse, M., *Catal. Today* **10**, 473 (1991).
14. Jian, M., and Prins, R., *Catal. Lett.* **50**, 9 (1998).
15. Singhal, G. H., Espino, R. L., Sobel, J. E., and Huff, G. A., *J. Catal.* **67**, 457 (1981).
16. Meille, V., Schulz, E., Lemaire, M., and Vrinat, M., *J. Catal.* **170**, 29 (1977).
17. Bataille, F., Lemberton, J. L., Michaud, P., Pérot, G., Vrinat, M., Lemaire, M., Schulz, E., Breysse, M., and Kasztelan, S., *J. Catal.* **191**, 409 (2000).
18. Moreau, C., Joffre, J., Saenz, C., Afonso, J. C., and Portefaix, J. L., *J. Mol. Catal. A* **161**, 141 (2000).
19. Jian, M., and Prins, R., *Catal. Today* **30**, 127 (1996).
20. Bachelier, J., Tilliette, M. J., Cornac, M., Duchet, J. C., Lavalley, J. C., and Cornet, D., *Bull. Soc. Chim. Belg.* **93**, 743 (1984).
21. Maugé, F., and Lavalley, J. C., *J. Catal.* **137**, 69 (1992).
22. Delgado, E., Fuentes, G. A., Hermann, C., Kunzmann, G., and Knözinger, H., *Bull. Soc. Chim. Belg.* **93**, 735 (1984).
23. Moreau, C., Joffre, J., Saenz, C., and Geneste, P., *J. Catal.* **81**, 168 (1983).
24. Pérot, G., Brunet, S., Canaff, C., and Toulhoat, H., *Bull. Soc. Chim. Belg.* **96**, 865 (1987).
25. Petit, C., Maugé, F., and Lavalley, J. C., *Stud. Surf. Sci. Catal.* **106**, 157 (1997).
26. Topsøe, N. Y., Topsøe, H., and Massoth, F. E., *J. Catal.* **119**, 252 (1989).
27. Topsøe, N. Y., and Topsøe, H., *J. Catal.* **139**, 641 (1993).
28. Leglise, J., Finot, L., van Gestel, J. N. M., Duchet, J. C., and Dubois, J. L., *Catal. Today* **45**, 347 (1998).
29. Mijoin, J., Thévenin, V., Garcia Aguirre, N., Yuze, H., Wang, J., Li, W. Z., Pérot, G., and Lemberton, J. L., *Appl. Catal. A* **180**, 95 (1999).
30. Kasztelan, S., Toulhoat, H., Grimblot, J., and Bonnelle, J. P., *Appl. Catal.* **13**, 127 (1984).
31. Müller, B., van Langeveld, A. D., Moulijn, J. A., and Knözinger, H., *J. Phys. Chem.* **97**, 9028 (1993).
32. Travert, A., Dujardin, C., Maugé, F., Cristol, S., Paul, J. F., Payen, E., and Bougeard, D., *Catal. Today*, in press.
33. Fraenkel, D., *Ind. Eng. Chem. Res.* **29**(9), 1814 (1990).
34. Lauritsen, J. V., Helveg, S., Lægsgaard, E., Stensgaard, I., Clausen, B. S., Topsøe, H., and Besenbacher, F., *J. Catal.* **197**, 1 (2001).